ORGANIC LETTERS

2009
Vol. 11, No. 20
4524−4527

Controlled Self-Assembly of Electron Donor Nanotubes

Juan Luis López,[†] Emilio M. Pérez,[†,‡] Pedro M. Viruela,[§] Rafael Viruela,[§] Enrique Ortí,[*,§] and Nazario Martín[*,†,‡]

Departamento de Química Orgánica, Facultad de Química, Universidad Complutense, 28040 Madrid, IMDEA-nanociencia, 28049 Madrid, Spain, and Instituto de Ciencia Molecular, Universidad de Valencia, 46980 Paterna, Spain

enrique.orti@uv.es; nazmar@quim.ucm.es

Received July 24, 2009

ABSTRACT

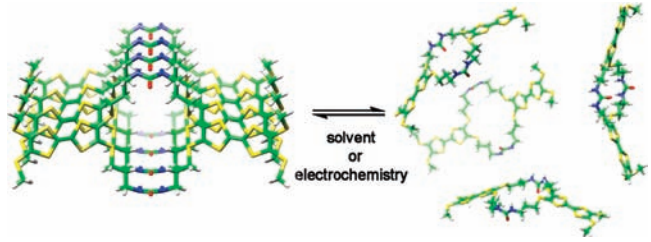

We employ a combination of urea−urea hydrogen bonds and $\pi-\pi$ stacking interactions to obtain soluble self-assembled nanotubes decorated with electron-donor TTF derivatives on the periphery. We have investigated the structure and stability of the nanotubes with a combination of experiments and high-level DFT calculations. We also demonstrate that the association process can be controlled by changes in the hydrogen-bonding ability of the solvent and electrochemically.

In the search for new materials for optoelectronic applications through self-assembly,[1,2] control over the assembly process and processability (i. e., solubility) of the supramolecules are two of the most sought-after characteristics. Recently, the Shimizu group has reported a series of bisurea macrocycles that self-assemble to form columnar nanotubes via a combination of strong urea−urea bifurcated hydrogen bonds and aromatic stacking interactions.[3] These macrocycles are highly symmetric—and thus synthetically affordable—and tolerant of structural modifications,[3a] so we reasoned they could be used to organize electroactive molecules in a controlled fashion. Although several other hydrogen-bonding motifs have been utilized for this purpose,[4] the bisurea macrocyclic system had remained unexplored, perhaps due to the characteristic lack of solubility of the aggregates. In this communication, we describe the synthesis of a bisurea

[†] Universidad Complutense.
[‡] IMDEA-nanociencia.
[§] Universidad de Valencia.

(1) (a) Yu, G.; Gao, J.; Hummelen, J. C.; Wudl, F.; Heeger, A. J. *Science* **1995**, *270*, 1789. (b) Halls, J. J. M.; Walsh, C. A.; Greenham, N. C.; Marseglia, E. A.; Friend, R. H.; Moratti, S. C.; Holmes, A. B. *Nature* **1995**, *376*, 498. (c) Zhang, X.; Chen, Z.; Würthner, F. *J. Am. Chem. Soc.* **2007**, *129*, 4886. (d) Janssen, P. G. A.; Vandenbergh, J.; Van Dongen, J. L. J.; Meijer, E. W.; Schenning, A. P. H. J. *J. Am. Chem. Soc.* **2007**, *129*, 6078.

(2) For examples involving TTF-type donors, see: (a) Canevet, D.; Sallé, M.; Zhang, G.; Zhang, D.; Zhu, D. *Chem. Commun.* **2009**, 2245. (b) Wang, C.; Zhang, D.; Zhu, D. *J. Am. Chem. Soc.* **2005**, *127*, 16372. (c) Pérez, E. M.; Illescas, B.; Herranz, M. A.; Martín, N. *New J. Chem.* **2009**, *33*, 228–234. (d) Fernández, G.; Sánchez, L.; Pérez, E. M.; Martín, N. *J. Am. Chem. Soc.* **2008**, *130*, 10674. (e) Fernández, G.; Pérez, E. M.; Sánchez, L.; Martín, N. *J. Am. Chem. Soc.* **2008**, *130*, 2410. (f) Fernández, G.; Pérez, E. M.; Sánchez, L.; Martín, N. *Angew. Chem., Int. Ed.* **2008**, *47*, 1094. (g) Pérez, E. M.; Sierra, M.; Sánchez, L.; Torres, M. R.; Viruela, R.; Viruela, P. M.; Ortí, E.; Martín, N. *Angew. Chem., Int. Ed.* **2007**, *46*, 1847. (h) Pérez, E. M.; Sánchez, L.; Fernández, G.; Martín, N. *J. Am. Chem. Soc.* **2006**, *128*, 7172.

(3) (a) Yang, J.; Dewal, M. B.; Sobransingh, D.; Smith, M. D.; Xu, Y.; Shimizu, L. S. *J. Org. Chem.* **2009**, *74*, 102. (b) Yang, J.; Dewal, M. B.; Shimizu, L. S. *J. Am. Chem. Soc.* **2006**, *128*, 8122. (c) Shimizu, L. S.; Hughes, A. D.; Smith, M. D.; Davis, M. J.; Zhang, B. P.; Zur Loye, H.-C.; Shimizu, K. D. *J. Am. Chem. Soc.* **2003**, *125*, 14972. (d) Shimizu, L. S.; Smith, M. D.; Hughes, A. D.; Shimizu, L. S. *Chem. Commun.* **2001**, 1592.

(4) (a) Young, E. R.; Rosenthal, J.; Hodgkiss, J. M.; Nocera, D. G. *J. Am. Chem. Soc.* **2009**, *131*, 7678. (b) Brea, R. J.; Castedo, L.; Granja, J. R.; Herranz, M. A.; Sánchez, L.; Martín, N.; Seitz, W.; Guldi Dirk, M. *Proc. Natl. Acad. Sci. U.S.A.* **2007**, *104*, 5291. (c) Murata, T.; Morita, Y.; Yakiyama, Y.; Fukui, K.; Yamochi, H.; Saito, G.; Nakasuji, K. *J. Am. Chem. Soc.* **2007**, *129*, 10837.

10.1021/ol901695m CCC: $40.75
Published on Web 09/16/2009

macrocycle bearing electron-donor di(methylthio)tetrathiafulvalene (DMTTF) groups and its solvent- and redox-controlled self-assembly into soluble organic nanotubes.

Early studies by Ranganathan et al. demonstrated that tubular assemblies were also obtained when utilizing flexible alkyl spacers between the urea groups.[5] The design of macrocycle **5** (Scheme 1) is based on this knowledge. **5**

Scheme 1. Synthesis of Macrocycle **5**

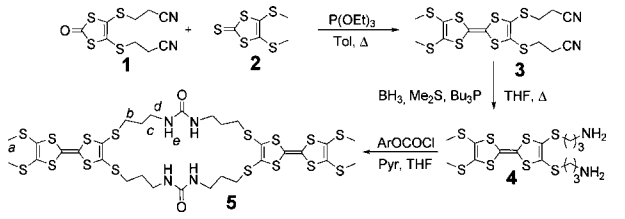

features two urea groups and two units of DMTTF, linked through alkyl spacers, that should permit assembly into nanotubes while improving solubility. The synthesis of **5** was carried out according to Scheme 1. Statistical coupling of **1** and **2** using $P(OEt)_3$ provided the DMTTF derivative **3**. Reduction of the nitrile groups of **3** through the use of a mixture of BH_3, Me_2S, and Bu_3P (10.5:10.5:10) in reflux of THF led to **4** in 62% yield. With amine **4** in our hands, macrocyclization was achieved through formation of mixed aromatic carbamates followed by in situ nucleophilic attack of the unreacted amines at a concentration of 7 mM. Macrocycle **5** and all synthetic intermediates were unambiguously characterized by standard spectrometric techniques.

Macrocycle **5** is sufficiently soluble in common organic solvents to allow for the study of its self-association in solution. Comparison of the room temperature ^{1}H NMR in $CDCl_3$, CD_3OD, d_7-DMF, and d_6-DMSO (Figure 1) provided evidence for the formation of oligomers of **5** through hydrogen bonding. In $CDCl_3$, a non-hydrogen-bond competing solvent ($\alpha_s = 2.2$, $\beta_s = 0.8$), **5** is only sparingly soluble, and its spectrum shows very broad signals for all protons except H_a. In CD_3OD ($\alpha_s = 2.7$, $\beta_s = 5.8$), all signals show the expected multiplicity. In d_7-DMF ($\alpha_s = 1.6$, $\beta_s = 8.3$), the signals corresponding to H_b, H_c, and H_d sharpen up, although not completely at room temperature. H_e appears at very low fields ($\delta = 8.7-8.9$ ppm) and shows a pattern indicative of the coexistence of H_e in different chemical environments, which are attributed to urea groups inside (more polarized, lower magnetic field) and at the ends of the associates. Integration of these leads to a ratio of approximately 10:1, which provides an idea of the length of the aggregates in this solvent. Finally, in the strong hydrogen bond acceptor d_6-DMSO ($\alpha_s = 0.8$, $\beta_s = 8.9$), H_{a-d} appear perfectly resolved. The chemical shift of H_e in this case is shifted upfield ($\delta = 7.9$ ppm) with respect to d_7-DMF, indicating that in d_6-DMSO the urea N−H bonds are less polarized. A plausible explanation for this is that in d_7-DMF strong, bifurcated urea−urea **5**•**5** hydrogen bonds are

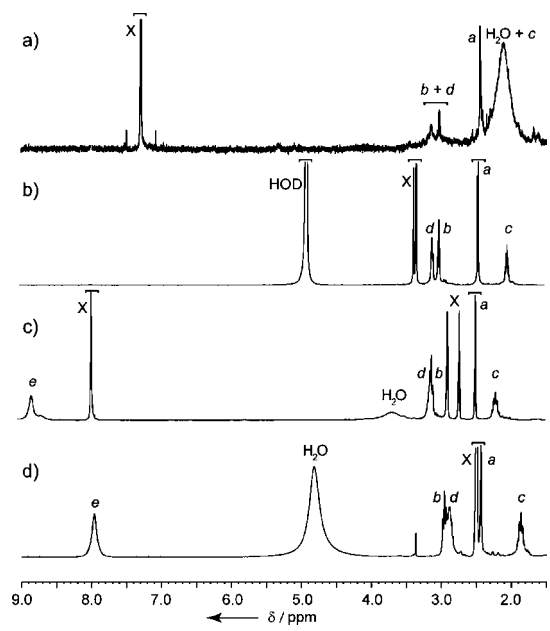

Figure 1. ^{1}H NMR spectra at 298 K of **5**: (a) $CDCl_3$, 500 MHz; (b) CD_3OD, 300 MHz; (c) d_7-DMF, 300 MHz; (d) d_6-DMSO, 300 MHz. The assignment corresponds to the lettering shown in Scheme 1. Solvent peaks are marked with an X.

dominant, whereas in d_6-DMSO hydrogen bonds of **5** with the solvent prevail.

To gain insight into the stability of the associates, we carried out variable-temperature NMR experiments in d_7-DMF (Figure S1, Supporting Information). Upon lowering temperature, broadening of H_{a-d} and slight deshielding of the H_e protons (-1.28 ppb K^{-1}) were the only changes observed. These data confirm that at room temperature most urea protons are involved in hydrogen bonding and not exposed to the solvent.[6]

Dilution experiments in d_7-DMF did not result in significant changes in the ^{1}H NMR spectrum of **5**. We attempted to disrupt the multimers by addition of d_6-DMSO to a 4.5 mM solution of **5** in d_7-DMF. The results of this denaturalization experiment are shown in Figure S2 (Supporting Information). We observed the progressive shielding of H_e, which in 70% d_6-DMSO finally leads to the convergence of the two signals observable in d_7-DMF. As a consequence of the well-known cooperative character of the self-association of ureas, disruption of the ensembles requires overcoming an activation barrier: up to ~40% d_6-DMSO, only small changes are observed, and from then on, rapid shielding of H_e occurs. All these data point to the existence of tightly associated, kinetically stable multimers of **5** in $CDCl_3$, whereas an n-mer/monomer exchange equilibrium is apparent

(5) Ranganathan, D.; Lakshmi, C.; Karle, L. I. *J. Am. Chem. Soc.* **1999**, *121*, 6103.

(6) The use of temperature coefficients is a long-known method for determining solvent exposure in protein conformation analysis by NMR. Typically, a temperature dependence of NH protons <3 ppb K^{-1} in hydrogen bond accepting solvents is considered an indication of them being hydrogen bonded and not exposed to solvent. See: Stern, A.; Gibbons, W. A.; Craig, L. C. *Proc. Natl. Acad. Sci. U.S.A.* **1968**, *61*, 734.

in all other solvents. Dynamic light scattering (DLS) measurements (Figure S3, Supporting Information) on solutions of **5** in CH_3OH (1.0×10^{-4} M, 298 K) were carried out to obtain a direct estimation of the length of the oligomers. A relatively broad distribution ranging from 110 to 150 nm and centered at 135 nm is observed.

The preferred mode of association of symmetrical bisurea macrocycles such as **5** is the formation of columnar assemblies.[3a,5] Nevertheless, we decided to investigate the geometry of the ensembles in solution. To do so, we took advantage of the presence of the electroactive DMTTF groups and carried out cyclic voltammetry (CV) and differential pulse voltammetry (DPV) experiments. Voltammograms were recorded for 5×10^{-5} M solutions of **5** in anhydrous and degassed DMF. The results are shown in Figure 2. Two different quasi-reversible and one irreversible

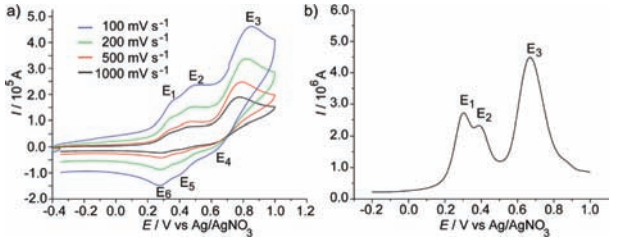

Figure 2. (a) Cyclic voltammograms of **5** (5×10^{-5} M, DMF, $Ag/AgNO_3$ as reference electrode, glassy carbon as working electrode, Bu_4NClO_4 as supporting electrolyte, 298 K) at several scan rates. (b) Differential pulse voltammetry of **5** under identical conditions.

oxidation processes can be observed. The first and third oxidation potentials—$E_1 = 0.30$ V and $E_3 = 0.67$ V from DPV experiments—are characteristic of the formation of the radical cation $DMTTF^{+\cdot}$ and dication $DMTTF^{2+}$. The appearance of a third oxidation process of intermediate potential, $E_2 = 0.39$ V, and the broadening of all waves are diagnostic of tetrathiafulvalene moieties being forced to stay in close spatial proximity.[7] This requirement can only be met if the macrocycles self-assemble to form nanotubes, where the DMTTF would be stacked, since an offset-type geometry[3a] would not permit approximation of the electroactive units.[8] Upon disruption of the supramolecular structure of $(\mathbf{5})_n$ by addition of DMSO, E_2 is no longer observable (Figure S4, Supporting Information).

Unfortunately, the gain in solubility provided by the alkyl chains renders **5** a noncrystalline solid. Thus, we carried out density functional theory (DFT) calculations at the MPWB1K/6-31G** level[9] to investigate the structure and stability of the multimers. In a first approximation, the flexibility of **5** allows for a great variety of conformations of the monomer (Figure S5, Supporting Information), among which the most stable in the gas phase consistently shows intramolecular hydrogen bonds (Figure 3a). As this conformation would

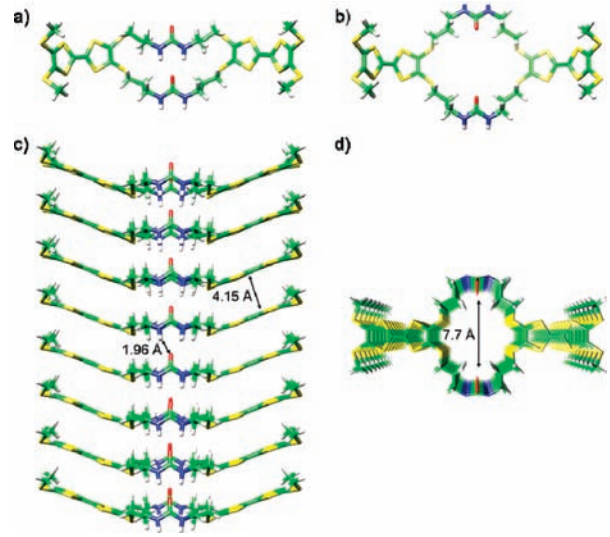

Figure 3. (a) and (b) Minimum-energy MPWB1K/6-31G** structures calculated for **5**. (c) and (d) Top and side views of the nanotubes $(\mathbf{5})_n$, showing eight repeating units and some key distances.

prevent the formation of oligomers, we forced the monomer to adopt a conformation where the hydrogen bonding groups are available for nanotube growth (Figure 3b). This conformation was also characterized as a minimum in the potential energy surface, and it has an energetic cost of 6.40 kcal mol^{-1}. This cost is greatly diminished in polar solvents, and the monomer structure without intramolecular hydrogen bonds is more stable by 1.06 kcal mol^{-1} in CH_3OH (1.35 kcal mol^{-1} in DMSO). Utilizing this conformation of **5** as a building block, we optimized the structure of the nanotubes as infinite 1D periodic systems; that is, we minimized the energy of a $(\mathbf{5})_n$ aggregate, where $n = \infty$.[10] In these calculations, both the geometry of the monomers and the intermolecular distances are optimized simultaneously (Figure 3c, 3d, and S6). In the nanotubes, **5** adopts a boat-like conformation, in which the DMTTF groups are slightly folded in a chair conformation (average folding along S···S axes = 7.2°) to accommodate the methyl groups, while allowing for the DMTTF moieties to stack efficiently (DMTTFs interplane distance = 4.15 Å, unit cell distance = 4.45 Å) in a face-to-face slipped manner. To keep the DMTTFs stacked, the urea groups adopt a parallel disposition, where both ureas of **5** point in the same direction. The average intermolecular H−O distance is 1.96 Å, in the range of strong hydrogen bonds and in good agreement with X-ray data on related systems.[3] The nanotubes

(7) (a) Aprahamian, I.; Olsen, J.-C.; Trabolsi, A.; Stoddart, J. F. *Chem.—Eur. J.* **2008**, *14*, 3889. (b) Lyskawa, J.; Sallé, M.; Balandier, J.-Y.; Le Derf, F.; Levillain, E.; Allain, M.; Viel, P.; Palacin, S. *Chem. Commun.* **2006**, 2233. (c) Yoshizawa, M.; Kumazawa, K.; Fujita, M. *J. Am. Chem. Soc.* **2005**, *127*, 13456.

(8) Folding of the macrocycle to approximate the two TTF units intramolecularly was proven to be energetically prohibitive. See the calculations section in the Supporting Information.

(9) (a) Zhao, Y.; Truhlar, D. G. *J. Phys. Chem. A* **2005**, *109*, 5656. (b) Zhao, Y.; Truhlar, D. G. *J. Chem. Theory Comput.* **2005**, *1*, 415. (c) Zhao, Y.; Truhlar, D. G. *J. Phys. Chem. A* **2004**, *108*, 6908.

(10) (a) Kudin, K. N.; Scuseria, G. E. *Chem. Phys. Lett.* **1998**, *289*, 611. (b) Kudin, K. N.; Scuseria, G. E. *Chem. Phys. Lett.* **2000**, *61*, 16440.

show a relatively small cavity of diameter 7.4−7.9 Å (H−H distance−S−S distance).

Notably, the calculations reproduce the cooperative association model suggested by the experimental ^{1}H NMR data. Figure S7 (Supporting Information) depicts the enhancement in stabilization of the nanotubes with increasing number of monomer units. As the associate grows, the hydrogen bonding network strengthens due to the larger polarization, and the associate becomes more stable. It is worth noting that the asymptotic limit ($n = \infty$) is rapidly approached upon addition of 8−12 monomer units, the increase in stabilization being relatively small from then on. Again, this is in perfect agreement with the ^{1}H NMR data in d_7-DMF. When $n = \infty$, the stabilization of the columnar nanotube per monomer unit with respect to the isolated monomer reaches 22.9 kcal mol^{-1}.

With this model in mind, we went on to investigate the possibility of controlling the self-assembly process electrochemically. To do so, we carried out CV experiments at different scan rates (100−1000 mV s^{-1}, Figure 2a). The electrochemical irreversibility of the third oxidation process is at first glance unexpected for this kind of TTF-based redox-active unit. Moreover, the potential at which the first reduction of the fully oxidized $\mathbf{5}^{4+}$ species occurs (E_4) is highly dependent on the scan rate. At slow scan rates (100 mV s^{-1}), it is difficult to visualize E_4. Instead, several low intensity waves are apparent. On increasing the scan rate, E_4 becomes distinguishable and is shifted to lower positive potentials, approximating reversibility. The redox behavior can be explained following a mechanism as that shown in Scheme 2. In a first oxidation process (E_1) involving n electrons—where n is the number of molecules of **5** that form part of the nanotube-mixed-valence species—$(\mathbf{5})^{n+}{}_n$ would be formed, in which charge-transfer interactions between vicinal oxidized and neutral DMTTF units would further stabilize the associates.[7] A second, more energetic oxidation, again involving n electrons, would take place at E_2 to afford species of the type $(\mathbf{5})^{2n+}{}_n$. Finally, full oxidation of $(\mathbf{5})^{2n+}{}_n$ takes place at E_3, a process which would involve $2n$ electrons and would yield $n \times \mathbf{5}^{4+}$ free macrocycles, due to Coulombic repulsion. Reduction of $n \times \mathbf{5}^{4+}$ to form $(\mathbf{5})^{2n+}{}_n$ takes place at E_4 and requires formation of the nanotubes. This is why the process becomes more irreversible at slower scan rates, where the free $\mathbf{5}^{4+}$ have had time to diffuse away from one another. The relative intensities E_1/E_3 and E_2/E_3 (Figure 2b) also support this image.

In conclusion, we have demonstrated how the reversible self-organization of electron−donor tetrathiafulvalene derivatives into supramolecular nanotubes can be achieved through a combination of urea−urea hydrogen bonds and $\pi-\pi$ stacking. The self-assembled nanotubes are soluble in most common organic solvents, and their degree of association is responsive to changes in solvent polarity and to electrochemical stimulation which makes them good candidates for their incorporation into opotoelectronic devices. To the best of our knowledge, this is the first time the well-known self-assembly properties of bisurea macrocycles are exploited to achieve ordered electroactive nanostructures.

Scheme 2. Proposed Redox-Controlled Assembly−Disassembly Mechanism

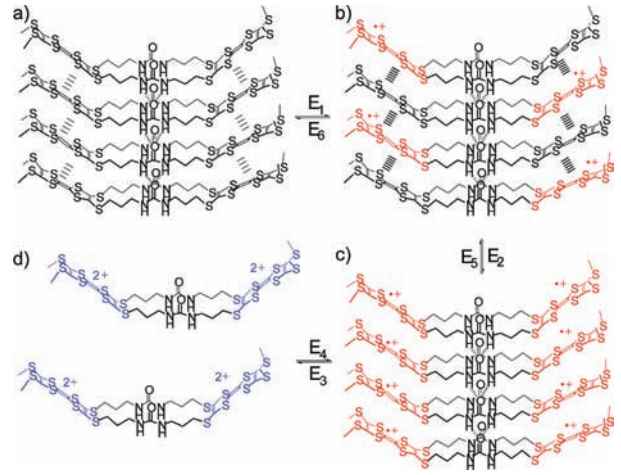

Acknowledgment. Financial support by the MICINN of Spain (CTQ2008-00795/BQU, CTQ2006-14987-C02-02/BQU, and CSD2007-00010), the CAM (MADRISOLAR project P-PPQ-000225-0505), the Generalitat Valenciana (ACOMP/2009/269), and European FEDER funds is acknowledged. J.L.L. thanks the Fundación Séneca, CARM of Spain, for a postdoctoral fellowship. E.M.P. thanks the MICINN for a Ramón y Cajal fellowship, cofinanced by the European Social Fund.

Supporting Information Available: Experimental and computational details and supplementary figures. This material is available free of charge via the Internet at http://pubs.acs.org.

OL901695M